Comparison of healing in forelimb and hindlimb surgically induced core lesions of the equine superficial digital flexor tendon

R. J. Estrada[1,2]; P. R. Van Weeren[3]; C. H. A. Van de Lest[3,4]; J. Boere[3]; M. Reyes[5]; J. C. Ionita[6]; M. Estrada[2]; C.J. Lischer[1]

[1]Equine Clinic, School of Veterinary Medicine, Free University of Berlin, Berlin, Germany; [2]Large Animal Hospital, School of Veterinary Medicine, National University, Heredia, Costa Rica; [3]Department of Equine Sciences, Faculty of Veterinary Medicine, Utrecht University, Utrecht, The Netherlands; [4]Department of Biochemistry and Cell Biology, Faculty of Veterinary Medicine, Utrecht University, Utrecht, The Netherlands; [5]Department of Orthopaedics, Erasmus MC, University Medical Center, Rotterdam, The Netherlands; [6]Large Animal Clinic for Surgery, Faculty of Veterinary Medicine, University of Leipzig, Leipzig, Germany

Keywords
Horse, superficial digital flexor tendon, tendinopathy, model, healing

Summary

Objective: Even though equine multi-limb tendinopathy models have been reported, it is unknown if fore- and hindlimb tendon healing behave similarly. The aim of this study was to compare the healing process of surgically induced superficial digital flexor tendon (SDFT) core lesions of fore- and hindlimbs in horses.

Methods: Tendon core lesions were surgically induced in the SDFT of both fore- and hindlimbs in eight horses. One randomly assigned forelimb and one randomly assigned hindlimb were injected with saline one and two weeks post-surgery. The healing process was monitored clinically and ultrasonographically. After 24 weeks, the tendons were harvested and biochemical, biomechanical and histological parameters were evaluated.

Results: Twenty-four weeks post-surgery, the forelimb SDFT lesions had a significantly higher colour Doppler ultrasound vascularization score ($p = 0.02$) and glycosaminoglycan concentration ($p = 0.04$) and a significantly lower hydroxylysylpyridinoline content ($p = 0.03$).

Clinical relevance: Our results indicate that fore- and hindlimb SDFT surgically induced lesions exhibit significant differences in several important parameters of tendon healing 24 weeks post-surgery. These differences create significant challenges in using all four limbs and accurately interpreting the results that one might generate. Therefore these findings do not support the use of four-limb models for study of tendon injury until the reasons for these differences are much better understood.

Correspondence to:
Roberto Estrada, DVM
Equine Clinic
Free Universtiy of Berlin
Oertzenweg 19b
14163 Berlin
Germany
Phone: +49 30 838 622 99
Fax: +49 30 838 625 29
E-mail: restrada@zedat.fu-berlin.de,

Vet Comp Orthop Traumatol 2014; 27: ••–••
http://dx.doi.org/10.3415/VCOT-13-11-0136
Received: November 13, 2013
Accepted: July 7, 2014
Epub ahead of print:

Introduction

Tendon pathologies are among the most common musculoskeletal disorders in horses (1). Some tendons are more prone to injury than others and the superficial digital flexor tendon (SDFT) is one of the most commonly affected structures (1–4). Tendon lesion distribution varies between horses engaged in the different equestrian disciplines, but in general SDFT lesions affect the forelimbs more often than the hindlimbs (1, 3, 4). Several studies have determined that peak vertical force and the associated stresses on the internal structures of the distal portion of the limb are higher in the forelimbs, leading to the suggestion that limb load distribution may play an important role in the development of musculoskeletal disorders in the horse (5-8). The authors of an *in vivo* study have proposed that biomechanical loading of tendons is involved in the initial enlargement of lesions (9). It is therefore conceivable that the differences in the load distribution and kinematics between fore- and hindlimbs might elicit different responses to tendon lesions in terms of lesion development, propagation and healing.

Several experimental models of equine SDFT tendinopathy have been developed; these are aimed at gaining a better understanding of the tendon healing process through the study of the response to artificially created lesions (10–13). These models have also been used to determine the effect of different therapeutic approaches to

tendon healing and to evaluate the effect of diagnostic analgesia (14-16). The models have traditionally been used in forelimb SDFT, since, as previously mentioned, natural lesions more often affect them and because both forelimbs are subject to similar biomechanical loads. Recently, a quadrilateral equine SDFT lesion model was reported in which lesions were induced in the SDFT of both fore- and hindlimbs and then randomly assigned to treatments using different therapeutic modalities (17). If fore- and hindlimb SDFT lesions have a similar healing pattern, it would make this model attractive for certain types of evaluations. However, for studies investigating therapies that have the potential for cross-over effects from one limb to another due to systemic effects or cell migration, this multi-limb model may not be a suitable choice. The recent use of multi-limb equine tendinopathy models calls for further investigation to determine if the healing of SDFT lesions in fore- and hindlimb are comparable.

The aim of this study was to compare the development (by ultrasonographic monitoring) as well as the outcome (based on biochemical, biomechanical and histological parameters) of standardized, surgically induced, SDFT core lesions of fore- and hindlimbs in horses. We hypothesized that there would be significant differences in the propagation and healing pattern between fore- and hindlimb SDFT lesions that would preclude direct comparison between fore- and hindlimbs when using this experimental model.

Table 1 Exercise regimen of the horses after quadrilateral lesion induction of the superficial digital flexor tendons.

Weeks post lesion induction	Walk (min/day)	Trot (min/day)
1–3	-	-
4–6	10	-
7–10	20	-
11–14	30	-
15–20	40	-
21–22	35	5
23–24	30	10

Materials and methods

This study was part of a larger research project in which the effect of an autologous platelet concentrate on tendon healing was compared to saline control (18). The present study used data derived from saline-treated fore- and hindlimb SDFT lesions only.

Experimental animals

This study was approved by the Bioethical and Animal Welfare Committee, School of Veterinary Medicine, National University, Costa Rica. Eight 2.5– to six-year-old mixed breed horses (average weight of 434 ± 38 kg) were selected for this study. The animals were free of lameness and did not exhibit any clinical or ultrasonographic signs of acute or chronic injuries of the SDFT in any of the four limbs. The horses were housed in individual boxes, fed a maintenance ration of concentrate with hay and had free access to water.

Lesion induction

All surgical procedures were performed while the horses were under general anaesthesia. The horses were sedated with xylazine[a] (1.1 mg/kg bodyweight [bwt] IV) and then anaesthetized using ketamine and midazolam[b] (2.2 mg/kg bwt IV). Thereafter, the anaesthesia was maintained using an isoflurane[c] based closed circuit. Core lesions in the SDFT of all fore- and hindlimbs were created using an adaptation of a previously described surgical model (11). In brief, a linear array multi-frequency probe[d] covered with a sterile palpation sleeve was used to identify the incision site, just proximal to the proximal recess of the digital flexor tendon sheath. A 1.5 cm skin incision was performed in the selected site using a No. 10 scalpel blade and then a stab incision was made through the paratendon with a No. 15 scalpel blade. Using ultrasonographic guidance, an inactivate disposable sideways-cutting 3.5 mm motorized synovial resector[e] was introduced proximally using manual pressure into the core of the tendon over a length of 7 cm. Once in position, the synovial resector was activated and slowly removed in approximately 20 seconds while repeatedly rotating the handpiece 180° in clockwise and counterclockwise directions. The paratendon and skin were closed using a simple interrupted suture pattern.

Postoperative care

The animals were treated with phenylbutazone[f] (2.2 mg/kg bwt p.o. twice daily) and penicillin-streptomycin[g] (1 ml/25 kg bwt IM once daily) one hour preoperatively and for three days postoperatively. Moreover, the horses were box-rested and the distal limbs were immobilized using a regularly changed Robert Jones bandage for three weeks. From week four onwards, a controlled exercise program was initiated (▶Table 1). The vital parameters, weight bearing, presence of lameness at walk, local swelling and signs of sensitivity were monitored daily throughout the study. At week 24, the lameness was graded using the American Association of Equine Practitioners lameness score (19). The tendon tenderness was classified as absent (no reaction), mild (focal sensitivity without limb withdrawal), moderate (focal sensitivity with slow limb withdrawal), and severe (focal sensitivity with fast limb withdrawal) depending on the reaction of the horse to palpation.

Treatment protocol

Intra-lesional treatment was performed one and two weeks post-surgery. The animals were sedated using xylazine[a] (1.1 mg/kg bwt IV), the limbs were aseptically prepared and the injection site was desensitized using 1 ml of subcutaneous lidocaine[h]. The limbs were left and right randomized by coin toss and each pair of forelimbs

a Procin® Equus: Pisa Agroveterinarios, Hidalgo, Mexico
b Ketamid®: Holliday, San Isidro, Argentina
c Aerrane: Baxter International Inc, Deerfield, Illinois, USA
d DP 3300 Vet: Mindray, Shenzhen, China
e Razorcut™ Blade: Smith & Nephew, Andover, Massachusetts, USA
f Fenilbutazona: Lisan, San José, Costa Rica
g Pen-Strep: Norbrook, Newry, Ireland
h Lidocaína HCL 2%: Laboratorios Faryvet, Heredia, Costa Rica

and hindlimbs were injected either with 2.5 ml of an autologous platelet concentrate or 2.5 ml of sterile saline. A **clinician ((AUTHOR INITIALS?))** blinded to the treatment used ultrasonographic guidance to place a 20 G x **38 mm needle** into the core lesions. The injection was performed on the longitudinal plane in a plantaro-proximal-dorsodistal direction aiming at the proximal aspect of the lesions.

Greyscale ultrasonographic evaluation

A linear multi-frequency probe set at **10 MHz[a] ((what is superscript a here for?))** and a silicone standoff pad were used to perform the echographic follow-ups of the SDFT lesions at one, two, four, six, 10, 15 and 24 weeks post-surgery. The limbs were divided into transverse and longitudinal zones as previously described and the distance distal to the accessory carpal bone or calcaneal tuberosity was recorded for each zone (20). Re-examinations of every zone in each pair of fore- and hindlimbs were performed at the same distances. A semi-quantitative scoring system was used to grade the echogenicity and fibre alignment of the lesions (20). The lesion length (LL) was defined as the length from the most proximal to the most distal aspect of the lesion. The total tendon cross-sectional area (TT-CSA) was calculated summing the CSA of the SDFT in six different zones (1A to 3B). The total lesion cross-sectional area (TL-CSA), total echo-score (T-ES), and total fibre alignment score (T-FAS) of transverse zones containing a lesion were calculated for each tendon by summing the values of each parameters to get total values. The total lesion percentage (TL-%) was calculated as follows: (TL-CSA / TT-CSA)*100 (20). A clinician blinded to treatment performed the data acquisition, measurements and scoring of the images (RJE).

Intra-tendinous vascularization score

The intra-tendinous vascularization was scored using a previously described technique (21). Colour Doppler ultrasound scans were performed 24 weeks post-surgery. The limbs were scanned in a flexed position to relax the tendinous structures and therefore avoid the collapse of intra-tendinous vessels due to mechanical forces. The images were obtained using a multi-frequency linear array probe set[i] at 10 MHz and a machine setting suitable for low flow vessel detection (VEL/6.2MHz; 0 Db; 1,099 KHz PRF). The lesions were localized and scanned from lateral to medial on the longitudinal plane. The image sequences of each scan were stored and the frame with the highest vascularization was selected subjectively and then scored. Data acquisition and vascularization grading were performed by a clinician blinded to treatment (RJE).

Sample harvesting, handling and shipping

After 24 weeks the horses were humanely euthanized. A combination of xylazine[a] (1.1 mg/kg bwt IV) and ketamine-midazolam[b] (2 mg/kg bwt IV) was used to induce a deep anaesthetic plane; thereafter a bolus of an oversaturated magnesium sulphate solution (1 g/kg bwt IV) was administered. The SDFT were harvested immediately after the euthanasia via sharp transection just distal to the accessory carpal bone or calcaneal tuberosity proximally and at the palmaro-plantarodistal aspect of the fetlock distally using a No. 20 scalpel blade. Once dissected, the tendons were divided into different sections as previously reported (14). Briefly, a transverse 1 cm tendon slice was obtained 2 cm proximal to the scar of the synovial resector portal, which was still visible in all the cases. The core lesions were identified and a 4 mm punch directed longitudinally was used to harvest injured tissue only. These samples were divided in three sections that were lyophilized for 24 hours using a vacuum freeze-dryer and then used to perform the biochemical analysis. Proximal to the aforementioned slice, a 3 cm segment was harvested and divided through the centre of the lesion in two longitudinal sections. The half used for biomechanical tests was initially frozen at –80°C, then shipped to the laboratories using a dry shipper[j] at approximately –150°C and subsequently stored at –80°C until further processing. The other half used for histological evaluation was fixed in four percent formalin for 48 hours and placed in 96% ethanol for five days (14). These samples were then sequentially transferred through a series of solutions of increasing isopropyl alcohol concentration and then embedded in paraffin blocks.

Glycosaminoglycans and DNA quantification

The tendon samples were papain digested (0.1 IU/mg of dry weight [dwt]) at 56°C for 12 hours. A dilution of the papain digest of each tendon was used to perform the GAG and DNA assays. The quantification of the sulphated glycosaminoglycan was performed using the 1,9-dimethylmethylene blue dye assay (22). Shark chondroitin sulphate was used as a standard (0–100 µg/ml). After an incubation period, the plates were assessed on a microplate reader[k]. Total DNA was quantified by means of the reaction with fluorescent dye[l] (23). Salmon sperm DNA was used as a standard (0–20 µg/ml). The luminescence was measured using a fluorescence spectrometer[m]. In both cases the final results were expressed as µg/mg of dry weight tendon.

Degraded collagen, total collagen, and cross links quantification

The tendon samples were processed with α-chymotrypsin to digest the degraded collagen (24). Hydroxyproline concentrations in the supernatant (containing the degraded collagen) were determined after the reaction with chloramine T and dimethylaminobenzaldehyde (25). Results were calculated as previously described and expressed as a percentage of degraded collagen (24). After the α-chymotrypsin digest, the tendon explants (containing the intact collagen) were hydrolyzed at 110°C

i Acuson AntaresTM: Siemens AG, Berlin, Germany

j MVE Vapor Shipper: Chart Industries, Ohio, USA

k VersaMax™: Molecular Devices, California, USA

l **Hoechst 33258: COMPANY NAME & LOCATION**

m LS-50B: Perkin Elmer, Waltham, Massachusetts, USA

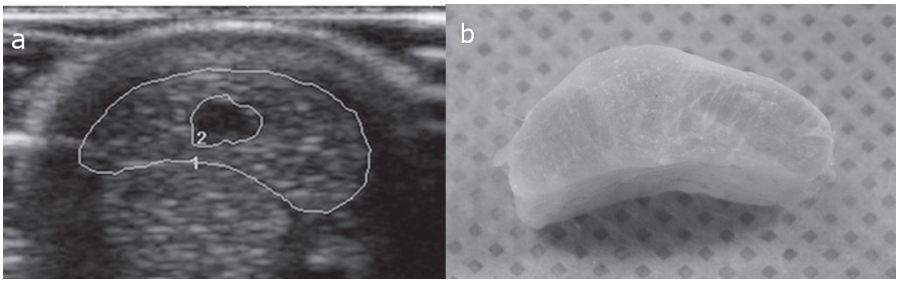

Figure 1 **a)** Surgically induced core lesion in a forelimb superficial digital flexor tendon (SDFT), 12 cm distal to the accessory carpal bone (zone 2B), four weeks post-surgery. **b)** Macroscopic view of a transverse slice of the same tendon 24 weeks post-surgery.

for 24 hours. The samples were vacuum dried for 24 hours, diluted in ultrapure water and centrifuged at 13,000 *g* for 20 minutes. The obtained supernatant was submitted to mass spectrometry, to determine the concentrations of hydroxyproline, hydroxylysylpyridinoline and lysylpyridinoline using a technique reported by Bosch and others (14). For calculation of the total collagen, the hydroxyproline content in the α-chymotrypsin digest supernatant was summed to the hydroxyproline of the explants measured with the mass spectrometry.

Pyrrole quantification

Pyrrole was quantified using a method adapted from a previously described technique (26). The freeze-dried tissues were minced, suspended in a pepsin/HCl solution and digested in a water bath at 45°C for 36 hours. Thereafter, the samples were centrifuged at 12,000 *g* for 15 minutes and 200 µl of supernatant were mixed with 40 µl of Ehrlich´s Reagent (4-dimethyaminobenzaldehyde, perchloric acid and deionized water) in a microplate. The samples were incubated at room temperature for 10 min and the absorbance was measured at 558 nm and 650 nm (non-related wavelength) in a microplate reader[i]. The pyrrole concentrations were calculated by comparison with a standard curve prepared by mixing 200 µl of 1-methyl-pyrrole (0–20 µmol/l) with 40 µl of Ehrlich´s Reagent. Results were expressed as mol per mol of collagen.

Biomechanical assessment

The biomechanical properties of the tendon samples were assessed using a modification of the method reported by others (14). The samples were thawed at room temperature. Longitudinal segments with an approximate cross section of 4 mm^2 and a length of 3 cm were cut from the core lesion of each tendon sample with a cutting device consisting of four disposable high profile microtome blades[n] at distances of 2 mm. A material testing machine[o] was used for failure testing. Sand paper was placed between the proximal and distal ends of the tendon sample and the clamps of the machine to decrease slippage. Once in position, the depth and width of the midsection of each sample were measured with a 0.01 mm resolution electronic caliper in a transverse plane to calculate cross-sectional area. The selected segments were tensed and preconditioned at 1 Hz and three percent strain for seven cycles and then tested to failure at a speed of 6 mm/min. The force at failure (F_{max}) and the stress-strain curve were determined for every sample. In each case the ultimate tensile strength was calculated (F_{max}/tendon cross-sectional area) and the elastic modulus deduced from the slope of the linear part of the curve (14)

Histology

Longitudinal 5 µm thick tendon sections were stained with Masson's trichrome[p]. Using this commercial histochemistry stain, the organized tendon collagen was stained red and disorganized collagen in the reparative tissue blue (10). Microphotographs of five consecutive fields of view (1x magnification) from different locations of each tendon samples were stored. At this magnification the complete thickness of the tendon section was observable in each microphotograph. An image manipulation software[q] was used to increase the contrast of the pictures. An image-processing package[r] was used to calculate the red/blue ratio of each histological section. Briefly, the images were assessed setting a threshold that allowed the isolation of the different stained areas in the histological section. Thereafter, the areas of interest (red / blue) were measured (27). The ratio between them was calculated per image and then the average red/blue ratio of the five images of each sample was calculated. The aforementioned colour ratio reflects the ratio between organized and disorganized collagen fibres. The evaluation of this parameter allows an indirect measurement of the overall degree of damage present in the tendon and therefore is a useful indicator of differences on tendon healing.

Statistical analysis

The data were analyzed using Excel[s] and Graph Pad Prism 6[t]. The D'Agostino-Pearson test was used to determine the data distribution. A paired Student's t-test was used to analyze the colour Doppler ultrasound vascularization score and the biochemical, biomechanical and histological parameters. After passing normality tests, the sonographic measurements were evaluated with repeated measures two-way ANOVA followed by a Bonferroni´s multiple comparison test. The sonographic scores showed a nonparametric distribution and therefore a Friedman test followed by Dunn´s multiple comparison test was applied. The signifi-

n Feather: Safety Razor Co. Ltd., Osaka, Japan
o Testometric AX M250 – 2.5 kN: Testometric Company, Lancashire, UK
p Artisan: Dako, Glostrup, Denmark
q Gimp 2.8: GNU Project, Free Software Fundation, Massachusetts, USA
r Fiji / ImageJ: National Institute of Health, Maryland, USA
s Excel: Microsoft Corporation, Washington, USA
t GraphPad Prism: GraphPad Software, California, USA

cance level was set at p ≤0.05. Results were reported as mean ± SD.

Results

Clinical assessment

All horses developed core lesions in their fore- and hindlimbs that resembled clinical and sonographic features of naturally occurring SDFT injuries (▶Figure 1). After lesion induction, horses were weight bearing normally at the stance, were not lame at the walk and showed signs of moderate to severe tenderness at palpation of the SDFT. No post-surgical complications were noted. After 24 weeks, six horses were sound at trot. Twenty-three weeks after treatment two horses had a grade 2/5 lameness (one forelimb and one hindlimb) and were therefore hand-walked for 10 min per day until the end of the study, instead of being subjected to the regular exercise protocol. The horse with the forelimb lameness showed signs of mild tendon tenderness in the lame forelimb at week 24. The other horse showed no signs of SDFT tenderness or other obvious reason that could explain the lameness.

Greyscale ultrasonographic evaluation

Pre-treatment (week 1), the sonographic parameters (TL-CSA [p = 0.64], TT-CSA [p = 0.18], TL-% [p = 0.40], LL [p = 0.61], T-ES [p = 0.61] and T-FAS [p = 0.59]) did not differ significantly when comparing fore- and hindlimbs. Post-treatment, even though the TL-CSA and TL-% of the forelimbs were greater and hindlimb lesion length larger, the sonographic parameters were not significantly different at any time point (▶Figure 2, ▶Figure 3).

Intra-tendinous vascularization scoring

The vascularization score (2.0 ± 1.3) for the forelimb SDFT was significantly higher than that of the hindlimbs (0.8 ± 1.1) 24 weeks post-surgery (p = 0.02) (▶Figure 4).

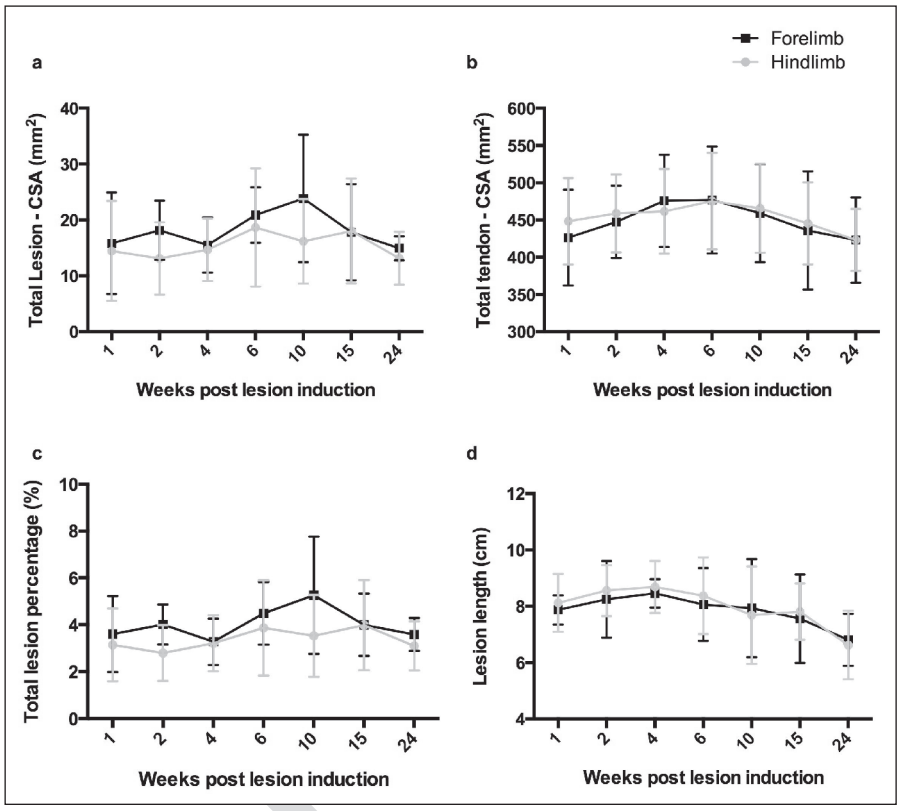

Figure 2 Greyscale ultrasonography measurements (mean ± SD) of saline-treated fore- and hindlimb surgically induced core lesions in the superficial digital flexor tendon followed-up over a 24-week period. **A)** Total lesion cross-sectional area (CSA), **B)** total tendon CSA, **C)** total lesion percentage, and **D)** lesion length.

Biochemical assessment

Twenty-four weeks post lesion induction, the forelimb SDFT lesions had a significantly higher glycosaminoglycan content (p = 0.04), whereas the hydroxylysylpyridinoline concentration in hindlimb SDFT lesions was significantly higher (p = 0.03). The DNA, total collagen, degraded collagen, lysylpyridinoline and pyrrole were not significantly different (▶Table 2).

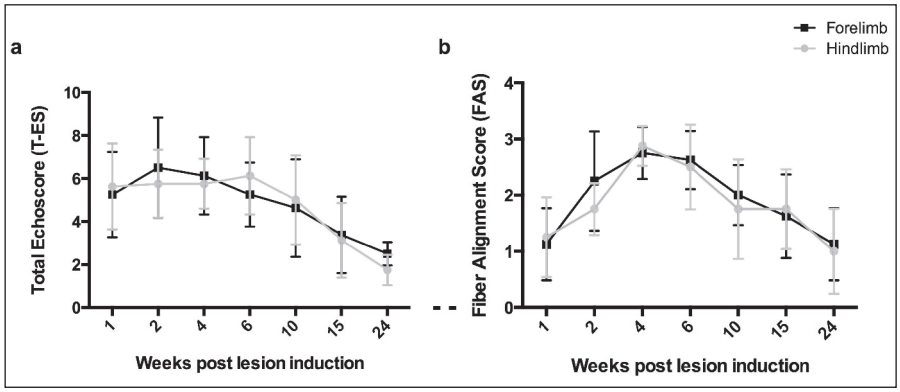

Figure 3 Greyscale ultrasonography semi-quantitative scores (mean ± SD) of saline-treated fore- and hindlimb surgically induced core lesions in the superficial digital flexor tendon followed-up over a 24-week period. **A)** Total echo score (T-ES) and **B)** fibre alignment score (FAS).

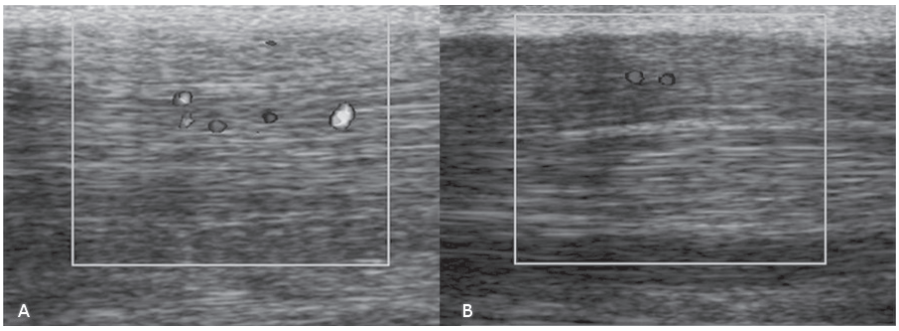

Figure 4 Vascularization of saline-treated fore- and hindlimb superficial digital flexor tendon (SDFT) lesions of the same horse 24 weeks after lesion induction detected with color Doppler ultrasound. Forelimb SDFT lesions **(A)** show a significantly higher vascularization score when compared to the hindlimb **(B)**.

Biomechanical assessment

There were no significant differences in the ultimate tensile strength (p = 0.53) or the elastic modulus (p = 0.27) when comparing the fore- and hindlimb SDFT. The data of three horses could not be compared since it was accidentally not stored in the system drive (▶Table 2).

Histology

There was no significant difference between the fore- and hindlimb red (organized collagen)/blue (reparative tissue) ratio of the histological images stained with Masson's trichrome (p = 0.55) (▶Table 2).

Discussion

This study showed that there were significant differences in tendon healing between fore- and hindlimb surgically induced core lesions treated with saline during the proliferative phase of healing. Twenty-four weeks after lesion induction, the vascularization score, sulphated glycosaminoglycan and hydroxylysylpyridinoline content were significantly different.

Tendons are multi-unit hierarchical structures mainly composed of collagen molecules (28). The intra- and intermolecular crosslinks are in part responsible for the physical properties of the tendinous collagen (29). Hydroxylysylpyridinoline is one of the major non-reducible collagen crosslinks found in the tendon (30). After tendon injury, the newly formed collagen within the lesion is less cross-linked than in normal tendons (31). During the remodelling phase, more stable crosslinks are formed resulting in repaired tissue with higher tensile strength and stiffness (32). In chronic tendinopathy, hydroxylysylpyridinoline is significantly increased when compared to healthy tendon, resulting in persistently high levels in the repaired tissue that affect the biomechanical properties of the tendon (33, 34). Glycosaminoglycans are polysaccharides that are usually covalently attached to core protein forming macromolecules known as proteoglycans (35). In tendons, glycosaminoglycans are in part involved in the regulation of the collagen fibrillogenesis, affecting fibril size and formation rate and contribute to the biomechanical and structural properties of the extracellular matrix (36, 37). The role of glycosaminoglycan accumulation after tendon damage is controversial. Previous studies in humans and horses indicate that degenerated tendon regions have higher concentrations of sulphated glycosaminoglycans (34, 38). Synthesis and accumulation of these molecules is usually correlated to an increased cellular metabolism within injured areas in the tendon and a marked increase of small collagen fibres, decreasing the mechanical properties of tendons and ligaments (38, 39). However, a recent study using blood products for the treatment of surgically induced core lesions interpreted the increase of intra-lesional sulphated glycosaminoglycan concentration as a positive feature of tendon healing when compared to saline-treated tendons (14). In the present study, 24 weeks after lesion induction, the hindlimb SDFT showed a significantly higher concentration of hydroxylysylpyridinoline and significantly lower concentration of sulphated glycosaminoglycans when compared to the forelimbs. The hy-

Table 2 Biochemical, biomechanical, and histological parameters (mean ± SD) of saline- treated fore- and hindlimb superficial digital flexor tendon lesions 24 weeks after lesion induction.

Parameters	Group		p-value
Biochemical	**Hindlimbs (n = 8)**	**Forelimbs (n = 8)**	
GAG – µg/mg dwt	18.1 ± 7.7	37.2 ± 24.8	0.04
DNA – µg/mg dwt	3.5 ± 1.4	3.4 ± 0.7	0.86
Total Collagen – mg/mg dwt	0.59 ± 0.1	0.63 ± 0.1	0.60
Degraded Collagen – %	0.75 ± 0.4	0.89 ± 0.6	0.54
Pyrrole – mol/mol collagen	0.06 ± 0.02	0.05 ± 0.01	0.40
HP – mol/mol collagen	0.68 ± 0.2	0.52 ± 0.1	0.03
LP – mol/mol collagen	0.02 ± 0.006	0.02 ± 0.005	0.48
Biomechanical	**Hindlimbs (n = 5)**	**Forelimbs (n = 5)**	
Ultimate Tensile Strength - MPa	18.3 ± 4.1	15.2 ± 9.4	0.54
Elastic Modulus - GPa	0.19 ± 0.04	0.15 ± 0.07	0.27
Histology	**Hindlimbs (n = 8)**	**Forelimbs (n = 8)**	
Masson's Trichrome Red / Blue Ratio – **Decimals**	0.12 ± 0.1	0.16 ± 0.1	0.55

GAG: glycosaminoglycans; HP: hydroxylysylpyridinoline; LP: lysylpyridinoline; dwt: dry weight.
AUTHORS – the meaning of "Decimals" above is unclear.

droxylysylpyridinoline concentration in the hindlimb lesions was close to the values previously reported for normal SDFT. Nevertheless, the sulphated glycosaminoglycan content was higher when compared to the same values (24). Together, the aforementioned findings suggest an ongoing healing process in both fore- and hindlimb SDFT. The less cross-linked tissue with higher concentration of sulphated glycosaminoglycans found in the forelimbs might be correlated to a relatively more immature reparative tissue.

As in other tissues, tendon lesions have an increased blood flow after acute injury, allowing cell recruitment and providing humoral mediators, growth factors and nutrients needed for adequate lesion healing (40). There is a general consensus that normal equine tendons have no detectable intra-tendinous blood flow when evaluated with colour or power Doppler ultrasound (21, 41). Persistent vascularization in tendinopathy has been interpreted as a sign of inadequate healing and incomplete repair (21, 41, 42). Recent preliminary studies in horses suggest that colour Doppler ultrasound could be a useful method for the differentiation between a more fragile vascular granulation tissue and hypovascular scar tissues during the remodelling phase of healing (42). Twenty-four weeks after lesion induction, the forelimb SDFT lesions showed a significantly higher colour Doppler ultrasound vascularization score. Hence the lower vascular density present in the hindlimb SDFT, where five out of eight horses showed no visible vascularization, can be interpreted as a positive step towards normalization of this parameter when compared to the forelimbs, and should theoretically be correlated to a more stable reparative tissue in the hindlimbs.

Interestingly, the significant differences in intra-tendinous vascularization, glycosaminoglycan, and hydroxylysylpyridinoline content were not correlated to significant differences in the ultimate tensile strength and elastic modulus when comparing fore- and hindlimbs. We believe that even though there were healing differences between fore- and hindlimb SDFT, the overall biomechanical characteristics of the tendons were not affected since other important biochemical parameters did not differ significantly.

Equine multi-limb tendinopathy models have been recently introduced as an option to compare the effect of different therapeutical modalities between the different limbs of the same animal (17). Nonetheless, it is not clear if the healing of fore- and hindlimb tendon lesions behave similarly. If fore- and hindlimb SDFT lesions have similar healing patterns, then the possibility of comparing different treatment modalities in the same animal would make this model attractive because of the decrease in animals needed and the increased number of tendons for analysis. However, for studies investigating therapies that have the potential for crossover effects from one limb to another due to systemic effects or cell migration, this multi-limb model may not be a suitable choice. Critics of this multi-limb approach have also raised concerns over animal welfare issues based on the potential for horses to have increased risk of infection, increased pain, and the inability to shift their weight off an injured limb. While these issues are certainly of significant concern and were taken into consideration when developing this model, we found that with the management used in this study, the horses did not show signs of infection or overt pain, neither directly after lesion induction nor throughout the study. Nonetheless, one can argue that pain was subjectively assessed and also pain in all four limbs would preclude them from exhibiting signs of discomfort in a particular limb.

The intra-lesional injection of saline might have influenced the natural healing process causing more local inflammation and fibre disruption due to distention of the lesion. This might have affected the tendon healing and therefore the final properties of the injured tissues. However, it is a current common practice to inject different therapeutic modalities into the SDFT core lesions and therefore these results may reflect modern practice better than a lesion that is left untreated. Moreover, all tendons were treated in the same fashion and so would affect lesions in fore- and hindlimbs equally.

There are several limitations to this study. Even though this particular surgical tendinopathy model successfully created repeatable lesions emulating several features of naturally occurring core lesions in the SDFT, it does not exactly replicate the chronic degenerative process that is believed to precede the majority of naturally occurring injuries (10, 34). Also, a period of 24 weeks is not long enough to evaluate the end-stage healing of the tendons, since the final maturation of tendon repair is usually reached after approximately one year (27). Several morphological parameters have been traditionally used to evaluate tendon healing by means of semi-quantitative scoring systems (14, 17). Aiming at objectivizing the evaluation, an image-processing package was used to analyze the histological sections of this study. Valuable information might have been lost due to the use of this technique alone. Even though the normal biochemical parameters of forelimb SDFT have been already published, processing healthy regions of the tendons would have allowed a more accurate comparison between the lesion site and the normal tissues (24). This is especially true for the hindlimb SDFT, where to the authors' knowledge, there are no reports of normal compositional parameters. Moreover, the low number of animals included might have negatively affected the power of this study.

In conclusion, our results indicate that fore- and hindlimb SDFT surgically induced lesions exhibit significant differences in several important parameters of tendon healing 24 weeks post-surgery. These differences create significant challenges in using all four limbs and accurately interpreting the results that one might generate. Therefore these findings do not support the use of four-limb models for study of tendon injury, until the reasons for these differences are much better understood.

Acknowledgements

The authors are grateful to J. Vargas, J.M. Estrada-McDermott, C. Murillo and the rotation students from the Large Animal Hospital and the Regenerative Therapy Unit, National University, Costa Rica for all their efforts during the course of this study. The authors are also grateful to R. Estrada, G. León and M. Herrera from the Clo-

domiro Picado Institute, Costa Rica for their help with sample preparation, to A. Castillo for facilitating sample export and to Prof. H. Weinans from the Orthopaedic Department, Erasmus MC for the advice with the biomechanical test. We would also like to thank Alimentos Montes de Oro and 3M, Costa Rica for the donation of concentrates and bandaging tape for this investigation.

Conflict of interest

No competing interests have been declared.

Source of funding

This project was financed by several parties: Arthrex Inc. (USA), the Equine Science Department at Utrecht University in Holland, and the Large Animal Hospital of the National University in Costa Rica. The living costs of the main author were financed by an ALECOSTA Scholarship.

References

1. Murray RC, Dyson SJ, Tranquille C, et al. Association of type of sport and performance level with anatomical site of orthopaedic injury diagnosis. Equine Vet J Suppl 2006; 36: 411–416.
2. Ely ER, Avella CS, Price JS, et al. Descriptive epidemiology of fracture, tendon and suspensory ligament injuries in National Hunt racehorses in training. Equine Vet J 2009; 41: 372–378.
3. Singer ER, Barnes J, Saxby F, et al. Injuries in the event horse: training versus competition. Vet J 2008; 175: 76–81.
4. Kasashima Y, Takahashi T, Smith RK, et al. Prevalence of superficial digital flexor tendonitis and suspensory desmitis in Japanese Thoroughbred flat racehorses in 1999. Equine Vet J 2004; 36: 346–350.
5. Back W, Schamhardt HC, Hartman W, et al. Kinematic differences between the distal portions of the forelimbs and hind limbs of horses at the trot. Am J Vet Res 1995; 56: 1522–1528.
6. Merkens HW, Schamhardt HC, van Osch GJ, et al. Ground reaction force patterns of Dutch Warmbloods at the canter. Am J Vet Res 1993; 54: 670–674.
7. Merkens HW, Schamhardt HC. Evaluation of equine locomotion during different degrees of experimentally induced lameness. I: Lameness model and quantification of ground reaction force patterns of the limbs. Equine Vet J Suppl 1988; 6: 99–106.
8. Merkens HW, Schamhardt HC. Evaluation of equine locomotion during different degrees of experimentally induced lameness. II: Distribution of ground reaction force patterns of the concurrently loaded limbs. Equine Vet J Suppl 1988; 6: 107–112.
9. David F, Cadby J, Bosch G, et al. Short-term cast immobilisation is effective in reducing lesion propagation in a surgical model of equine superficial digital flexor tendon injury. Equine Vet J 2012; 44: 570–575.
10. Cadby JA, David F, van de Lest C, et al. Further characterisation of an experimental model of tendinopathy in the horse. Equine Vet J 2013; 45: 642–648.
11. Schramme M, Hunter S, Campbell N, et al. A surgical tendonitis model in horses: technique, clinical, ultrasonographic and histological characterisation. Vet Comp Orthop Traumatol 2010; 23: 231–239.
12. Watkins JP, Auer JA, Gay S, et al. Healing of surgically created defects in the equine superficial digital flexor tendon: collagen-type transformation and tissue morphologic reorganization. Am J Vet Res 1985; 46: 2091–2096.
13. Williams IF, McCullagh KG, Goodship AE, et al. Studies on the pathogenesis of equine tendonitis following collagenase injury. Res Vet Sci 1984; 36: 326–338.
14. Bosch G, van Schie HT, de Groot MW, et al. Effects of platelet-rich plasma on the quality of repair of mechanically induced core lesions in equine superficial digital flexor tendons: A placebo-controlled experimental study. J Orthop Res 2010; 28: 211–217.
15. Dahlgren LA, van der Meulen MC, Bertram JE, et al. Insulin-like growth factor-I improves cellular and molecular aspects of healing in a collagenase-induced model of flexor tendinitis. J Orthop Res 2002; 20: 910–919.
16. Keg PR, Barneveld A, Schamhardt HC, et al. Clinical and force plate evaluation of the effect of a high plantar nerve block in lameness caused by induced mid-metatarsal tendinitis. Vet Q. 1994; 2: 70–75.
17. Crovace A, Lacitignola L, Rossi G, et al. Histological and immunohistochemical evaluation of autologous cultured bone marrow mesenchymal stem cells and bone marrow mononucleated cells in collagenase-induced tendinitis of equine superficial digital flexor tendon. Vet Med Int 2010; 2010: 250978.
18. ((ADD IN AUTHOR NAMES)). Effects of leukocyte-reduced platelet concentrate on the repair of surgically induced core lesions in equine superficial digital flexor tendon. BMC Vet Res 2014; Submitted for Publication ((IS THIS STILL UNDER REVIEW?)).
19. American Association of Equine Practitioners. Definition and classification of lameness. In: Guide for Veterinary Service and Judging of Equestrian Events. Lexington, KY, USA; American Association of Equine Practitioners, 1991.
20. Rantanen NW, Jorgensen JS, Genovese RL. Ultrasonographic Evaluation of the Equine Limb: Technique. In: Dyson S, Ross, editors. Diagnosis and Management of Lameness in the Horse. Vol 2. Missouri: Elsevier Saunders; 2011. pg. 183–205.
21. Bosch G, Moleman M, Barneveld A, et al. The effect of platelet-rich plasma on the neovascularization of surgically created equine superficial digital flexor tendon lesions. Scand J Med Sci Sports 2011; 21: 554–561.
22. Farndale RW, Sayers CA, Barrett AJ. A direct spectrophotometric microassay for sulphated glycosaminoglycans in cartilage cultures. Connect Tissue Res 1982; 9: 247–248.
23. Kim YJ, Sah RL, Doong JY, et al. Fluorometric assay of DNA in cartilage explants using Hoechst 33258. Anal Biochem 1988; 174: 168–176.
24. Lin YL, Brama PA, Kiers GH, et al. Functional adaptation through changes in regional biochemical characteristics during maturation of equine superficial digital flexor tendons. Am J Vet Res 2005; 66: 1623–1629.
25. Reddy GK, Enwemeka CS. A simplified method for the analysis of hydroxyproline in biological tissues. Clin Biochem 1996; 29: 225–229.
26. Thorpe CT, Stark RJ, Goodship AE, et al. Mechanical properties of the equine superficial digital flexor tendon relate to specific collagen cross-link levels. Equine Vet J Suppl 2010; 38: 538–543.
27. Jensen EC. Quantitative analysis of histological staining and fluorescence using ImageJ. Anat Rec (Hoboken) 2013; 296: 378–381.
28. Silver IA, Brown PN, Goodship AE, et al. A clinical and experimental study of tendon injury, healing and treatment in the horse. Equine Vet J Suppl 1983; 1: 1–43.
29. Tsuzaki M, Yamauchi M, Banes AJ. Tendon collagens: extracellular matrix composition in shear stress and tensile components of flexor tendons. Connect Tissue Res 1993; 29: 141–152.
30. Parry DA. The molecular and fibrillar structure of collagen and its relationship to the mechanical properties of connective tissue. Biophys Chem 1988; 29: 195–209.
31. Eyre DR, Koob TJ, Van Ness KP. Quantitation of hydroxypyridinium crosslinks in collagen by high-performance liquid chromatography. Anal Biochem 1984; 137: 380–388.
32. Williams IF, Heaton A, McCullagh KG. Cell morphology and collagen types in equine tendon scar. Res Vet Sci 1980; 28: 302–310.
33. Bank RA, Te Koppele JM, Oostingh G, et al. Lysylhydroxylation and non-reducible cross-linking of human supraspinatus tendon collagen: changes with age and in chronic rotator cuff tendinitis. Ann Rheum Dis 1999; 58: 35–41.
34. Birch HL, Bailey AJ, Goodship AE. Macroscopic 'degeneration' of equine superficial digital flexor tendon is accompanied by a change in extracellular matrix composition. Equine Vet J 1998; 30: 534–539.
35. Esko JD. Proteoglycans and Glycosaminoglycans. In: Varki A, Cummings R, Esko JD, editors. Essentials of Glycobiology [eBook]. Vol 2. New York: Cold Spring Harbor Laboratory Press; 1999. Available from: http://www.ncbi.nlm.nih.gov/books/NBK20693/
36. Cribb AM, Scott JE. Tendon response to tensile stress: an ultrastructural investigation of collagen:proteoglycan interactions in stressed tendon. J Anat 1995; 187: 423–428.
37. Parkinson J, Samiric T, Ilic MZ, et al. Involvement of Proteoglycans in Tendinopathy. J Musculoskelet Neuronal Interact 2011; 11: 86–93.
38. Parkinson J, Samiric T, Ilic MZ, et al. Change in Proteoglycan Metabolism Is a Characteristic of Human Patellar Tendinopathy. Arthritis Rheum 2010; 62: 3028–3035.

39. Halper J, Kim B, Khan A, et al. Degenerative suspensory ligament desmitis as a systemic disorder characterized by proteoglycan accumulation. BMC Vet Res 2006; 2: 12.
40. Yang X, Coleman DP, Pugh ND, et al. The volume of the neovascularity and its clinical implications in achilles tendinopathy. Ultrasound Med Biol 2012; 38: 1887–1895.
41. Kristoffersen M, Ohberg L, Johnston C, et al. Neovascularisation in chronic tendon injuries detected with colour Doppler ultrasound in horse and man: implications for research and treatment. Knee Surg Sports Traumatol Arthrosc 2005; 13: 505–508.
42. Murata D, Misumi K, Fujiki M. A preliminary study of diagnostic color Doppler ultrasonography in equine superficial digital flexor tendonitis. J Vet Med Sci 2012 74: 1639–1642.